Torques Responsible for Evolution of Atmospheric Angular Momentum during the 1982–83 El Niño

RUI M. PONTE AND RICHARD D. ROSEN

Atmospheric and Environmental Research, Inc., Cambridge, Massachusetts

(Manuscript received 17 June 1998, in final form 21 December 1998)

ABSTRACT

Atmospheric angular momentum (AAM) reached extremely high values during the large 1982–83 El Niño event. The mechanisms responsible for the anomalously high AAM are examined using mountain torque (τ_m) and friction torque (τ_f) time series computed from the National Centers for Environmental Prediction–National Center for Atmospheric Research reanalyses. AAM anomalies, defined with respect to a 29-yr climatology (1968–96), are mostly positive from mid-1982 onward, but notably they double in amplitude over a 2-week period in early 1983. Analysis of the torque series reveals that this sharp AAM increase is mostly related to anomalies in τ_m, primarily associated with American and Eurasian orography. After reaching its peak value in January, AAM anomalies decay slowly to near-normal values over the next three months, with anomalies in τ_f, especially over the subtropical North Pacific, playing a dominant role in this downturn. The relevant anomalies in τ_m and τ_f are discussed in relation to rapid synoptic-scale variability and longer-term, large-scale anomalous patterns in surface pressure and winds that characterized this El Niño event.

1. Introduction

In late January 1983, at the height of one of the largest El Niño events on record, observed values of axial atmospheric angular momentum (AAM)—more precisely the relative component associated with zonal winds—reached an all-time high (Rosen et al. 1984). The peak in AAM was associated with stronger than normal westerlies in the Tropics and subtropics and ultimately related to exchanges of angular momentum at the lower boundary, through either friction or mountain torques (e.g., Ponte et al. 1994). The torque mechanisms responsible for the observed AAM anomaly were, however, not easily determined given the available data. Rosen et al. speculated that the large-scale changes in pressure associated with the Southern Oscillation could provide the necessary anomalies in mountain torques associated with Eurasian and American orography to account for the AAM peak.

Since the original work of Rosen et al., two studies have tried to clarify the torques responsible for the evolution of AAM during the 1982–83 El Niño. Using available pressure data, Wolf and Smith (1987) examined the mountain torques over the Tibetan Plateau, the Rockies, and the Andes, for the period December 1982–February 1983, and found that the sharp rise in AAM in January 1983 could be mostly accounted for by torques on the Rockies related to a series of synoptic weather systems in the Pacific–North American region. The decrease in AAM that followed the January peak could not be explained by the mountain torques examined, however. Ponte et al. (1994) attempted a more comprehensive torque study but based on the Canadian Climate Centre model simulations of Boer (1985). Friction torques, which included the effects of gravity wave stresses as parameterized in the model, were found to be important for the slowly evolving model AAM anomalies, with mountain torque providing for more rapid signals in AAM. The relation with the observations was, however, not easily determined, as the model and observed AAM evolution differed in detail, particularly in early 1983.

The studies of Wolf and Smith (1987) and Ponte et al. (1994) raise many questions regarding the relative role of friction and mountain torques, as well as synoptic and more slowly evolving systems, in driving AAM tendencies during the 1982–83 El Niño. In addition, the relation between torque anomalies and the anomalous large-scale patterns in surface winds and pressure that accompanied the 1982–83 El Niño is still unclear. Such issues gain increased significance given the recent 1997–98 El Niño, comparable in many respects to the 1982–83 event. In this article, we take advantage of a recently computed torque dataset to readdress these questions. Our findings confirm the importance of the

Corresponding author address: Dr. Rui M. Ponte, Atmospheric and Environmental Research, Inc., 840 Memorial Drive, Cambridge, MA 02139-3794.
E-mail: ponte@aer.com

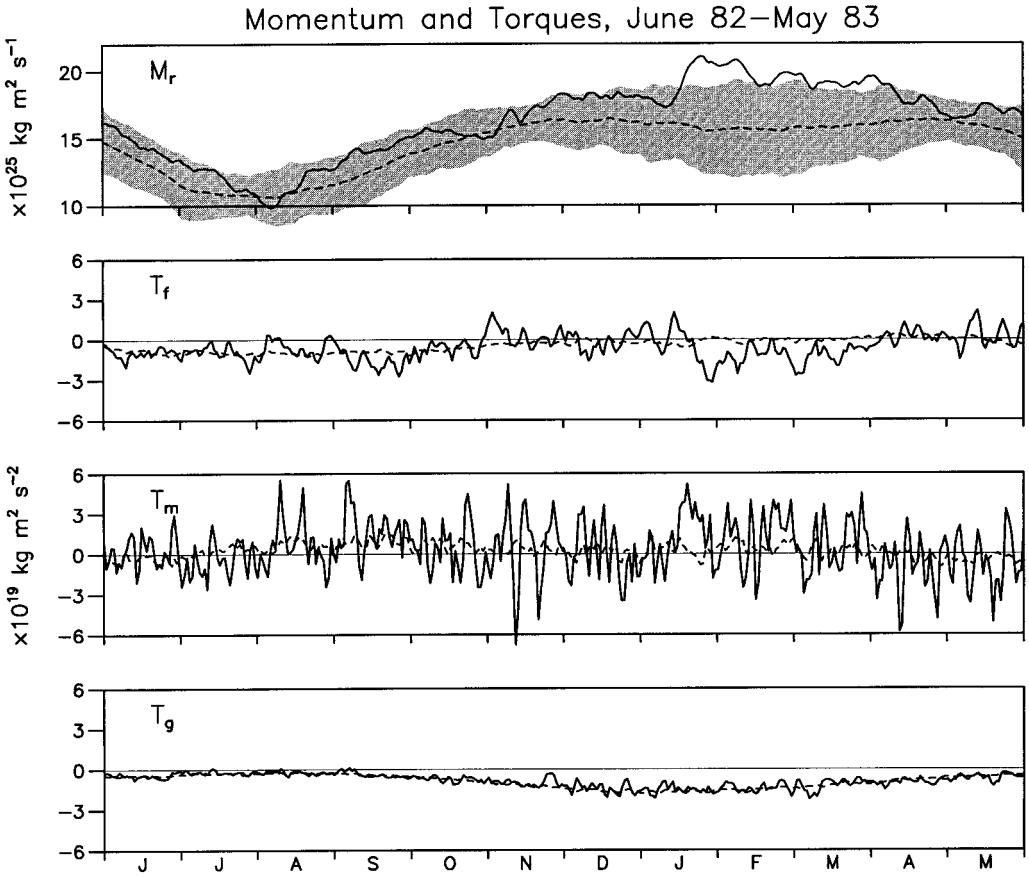

FIG. 1. Time series of daily averaged M_r, T_f, T_m, and T_g (from top to bottom), displayed as solid lines, for the 1-yr period starting on 1 Jun 1982, together with respective climatological means plotted as dashed lines. Shading around mean M_r curve represents anomalies smaller than ± 2 std dev.

mountain torque on the Rockies for the sharp AAM rise in January, as found by Wolf and Smith, but also reveal comparable contributions from mountain torques over Eurasia. Moreover, friction torques over the northern subtropics are found to be the dominant factor in bringing AAM down to normal levels by April 1983.

2. AAM and torques during 1982–83 El Niño

The reanalysis efforts at the National Centers for Environmental Prediction–National Center for Atmospheric Research (NCEP–NCAR) have produced a high-quality, multidecadal atmospheric dataset of demonstrated relevance for AAM studies (Salstein and Rosen 1997). Our AAM budget analysis is based on the NCEP–NCAR products covering the period 1968–96. The quantities involved are globally integrated relative angular momentum (M_r) and planetary angular momentum (M_Ω), associated with atmospheric zonal winds and solid body rotation, respectively, and gridded values of friction, mountain, and gravity wave torques (τ_f, τ_m, and τ_g). The notation is as in Ponte et al. (1994), with capital letters reserved for globally integrated quantities. Zonal winds up to the 10-hPa level and surface pressures were integrated globally to create 6-hourly values of M_r and M_Ω, respectively. The concurrent torque dataset was produced by K. Weickmann and collaborators at NOAA's Climate Diagnostics Center in Boulder (see, e.g., Huang et al. 1999). Values of τ_f and τ_m were evaluated from archived surface wind stresses and pressures, respectively, on an equally spaced grid in longitude (1.875°) and gaussian grid in latitude with similar resolution. Gravity wave torques, representing the effects of subgrid-scale orography on momentum flux at the land–atmosphere boundary, were also calculated based on the model parameterizations of such processes. While τ_m represents instantaneous values, τ_f and τ_g represent averaged values over respective 6-h intervals.

Given the negligible importance of changes in M_Ω to AAM variability and, in particular, to the El Niño anomalies, as discussed by Rosen et al. (1984) and others, focus here is on the evolution of M_r. The 6-hourly values for all quantities were averaged in time to create daily time series of M_r and of globally integrated friction, mountain, and gravity wave torques (denoted by T_f, T_m, and T_g, respectively). All four time series are shown in Fig. 1 for the 1-yr period from 1 June 1982 to 31 May 1983, coinciding with the period of the model analysis

by Ponte et al. (1994) and capturing the essential phases of the El Niño event under study. Also shown in Fig. 1 are climatological values of M_r, T_f, T_m, and T_g, obtained by averaging quantities at each sampling time over the 29 years of data available. The envelope of variability corresponding to ±twice the standard deviation of M_r about the climatological value is shown in Fig. 1 to allow for a quantitative assessement of the size of the El Niño M_r anomalies (δM_r).

Our focus is on the AAM and torque anomalies during the El Niño event. Therefore, the ensuing discussion and analysis do not address the nature of the climatological fields [see Huang et al. (1999) for a treatment of the full fields in a different context]. As discussed by previous works and confirmed by Fig. 1, AAM is characterized by above-normal values for much of the study period. The positive anomalies are interrupted only briefly in early August and late October. November marks the start of an uninterrupted 6-month period during which δM_r remains positive. The most significant upward trend in AAM occurs in January and takes AAM to its highest level in the NCEP–NCAR series, with δM_r values more than three standard deviations above the mean. Anomalies stay mostly above the two standard deviation threshold for the next two months but gradually diminish to near-normal values by the end of April.

Torques anomalies for the same period in Fig. 1 show two conspicuous signals that begin to reveal the processes responsible for the AAM evolution in early 1983. Anomalies in T_m (δT_m) typically change sign on weekly and shorter timescales. There is, however, a period of almost two weeks in January 1983 during which δT_m stays positive throughout. This period is associated with the strong upturn in δM_r. (A similar but weaker positive δT_m is observed also in the second half of February.) Anomalies in T_f (δT_f) vary on longer timescales than those of δT_m, confirming the different timescales at which T_f and T_m operate (Swinbank 1985; Boer 1990; Madden and Speth 1995). The most prolonged, conspicuous δT_f signal occurs from late January to April, when T_f shows persistent below-normal values, coinciding with the decline of M_r to near-normal values. Anomalies in T_g (δT_g) are typically much smaller than those in the other two torques. Figure 1 suggests, therefore, a complex interplay between T_m and T_f in shaping the evolution of AAM during the 1982–83 El Niño. This interplay is explored in more detail next.

3. AAM and time-integrated torque anomalies

To establish a quantitative relation between the anomalous torques and the evolution of AAM, we examine the relationship between δM_r and the time-integrated torque anomalies δT_f and δT_m. In general, one can write (e.g., Ponte et al. 1994)

$$\delta M(t) - \delta M(t_i) \approx \delta M_r(t) - \delta M_r(t_i) = \int_{t_i}^{t} \delta T_m \, dt + \int_{t_i}^{t} \delta T_f \, dt + \int_{t_i}^{t} \delta T_g \, dt + R, \quad (1)$$

where t_i is some relevant initial time, $M = M_r + M_\Omega$, and R is a residual mainly representing expected errors in the estimated torque and AAM quantities (Madden and Speth 1995; Huang et al. 1999). In (1), we have chosen to neglect δM_Ω compared to δM_r, so that the residuals will also incorporate the (small) effects of variable M_Ω. For simplicity in notation, we will denote $\delta M_r(t) - \delta M_r(t_i)$ by $\delta M_r'$. The equation expresses the conservation of anomalous AAM in the absence of sources and sinks represented by the torque anomalies on the right-hand side. Linking $\delta M_r'$ to the torque anomalies using (1) is straightforward using the NCEP–NCAR products. We shall carry in the analysis the residuals R to assess confidence in the observed signals in $\delta M_r'$ and their relation to the time integrals of δT_f, δT_m, and δT_g.

Given the discussion of Fig. 1, we focus the analysis on the period between January and April 1983, corresponding to the strongest upward trend and subsequent decay of M_r during the observation window. We also tried to examine the anomalous AAM behavior over the whole El Niño period, particularly from November onward (cf. Fig. 1), but these efforts led to ambiguous results, as small biases in the AAM budget yield comparatively large residual signals when integrated over many months. [See Huang et al. (1999) for a thorough analysis of the residuals in the AAM balance represented by the NCEP–NCAR products.] Concentrating first on the sharp rise in early 1983, we show in Fig. 2a the various quantities in (1) for the period January 11–23; the initial time chosen coincides with the start of the upward turn in M_r, and the end time coincides with the maximum in M_r. Contributions from T_f seem to be important for the increase in $\delta M_r'$ over the first 3 days. By 14 January, however, a strong positive trend in δT_m ensues, and contributions from δT_m shortly overtake those of δT_f, remaining clearly dominant through the end of the period (δT_f actually turns negative around 21 January and $\int \delta T_f \, dt$ in Fig. 2a starts to decrease). Effects of δT_g are very small and not important. Although not negligible, the residual in the AAM balance is small compared to the signals in $\delta M_r'$ or δT_m through the bulk of the period. Hence, the importance of δT_m signals to the rise in AAM seems to be a robust result.

To determine which regions are responsible for the observed δT_m, Fig. 2b shows the mountain torque calculated in four different boxes enclosing most major mountain ranges. Following Iskenderian and Salstein (1998), we focus on latitudinal bands 10°–50°S and 19°–60°N, where most variability in τ_m is found, and we break each band into two contiguous boxes with north–

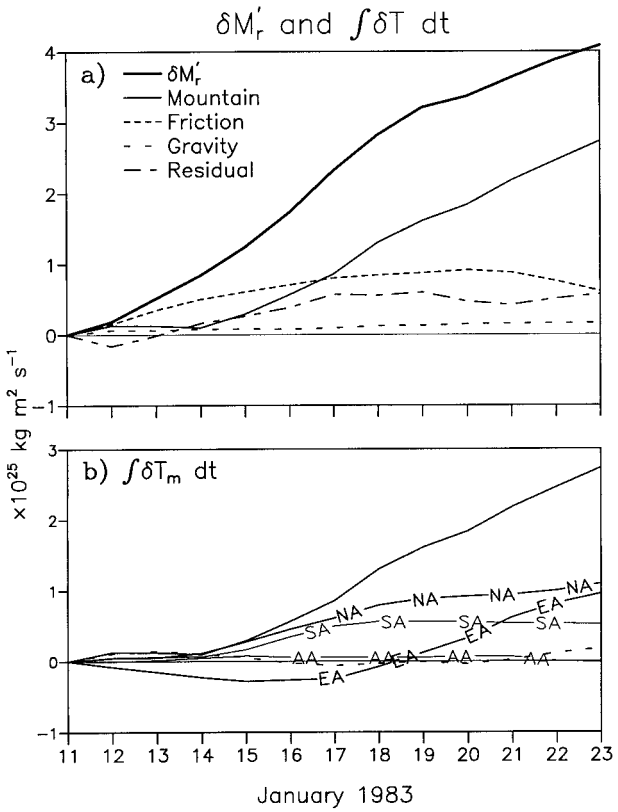

FIG. 2. (a) Time evolution of $\delta M_r'$, time-integrated mountain, friction, and gravity wave torque anomalies, and their residual, as defined by (1), for the period of sharp AAM rise in Jan 1983. (b) Evolution of time-integrated anomalies in δT_m (solid line, unlabeled), together with respective contributions from NA, SA, EA, and AA, and remainder (dashed) regions, as defined in the text.

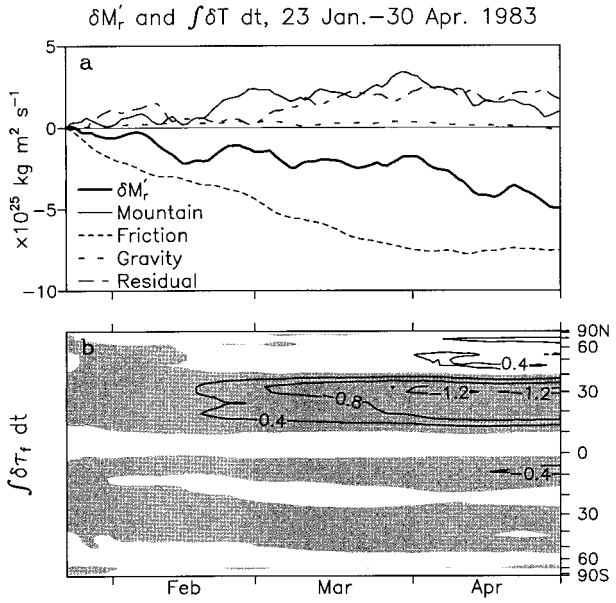

FIG. 3. (a) As in Fig. 2a but for the period marking the decline of M_r to near-normal values, from 23 Jan to the end of April 1983. (b) Hovmöller diagram in time and latitude of time-integrated, zonally averaged anomalies in τ_f, for the same period. Contour interval is 0.4×10^{25} kg m^2 s^{-1}; negative values are shaded.

south boundaries over the ocean. The Northern Hemisphere boxes enclose North America (NA) and Eurasia (EA), while the Southern Hemisphere boxes enclose South America (SA) and Africa–Australia (AA). North America, South America, and Eurasia boxes mainly represent mountain torques on the Rockies, Andes, and the Tibetan Plateau, respectively. Figure 2b indicates that torques on NA seem especially important during 14–19 January, while torques on EA contribute a negative trend until 17 January, but by the end of the period become as important a factor as NA in the increase of $\int \delta T_m\, dt$. Torque anomalies on SA are comparable to those on NA until 17 January, but are half those on NA and EA when their cumulative effect is considered at the end of the period. Torque on AA is negligible, as is the remainder torque from regions not included in NA, EA, SA, and AA, also shown in Fig. 2b. In summary, the January peak in AAM involves largely mountain torques on NA and EA orography, with initial help from anomalous mountain torques on SA and also δT_f.

The slow decline of M_r to near-normal values, initiated after the peak on 23 January, is examined in Fig. 3. While δT_m continues to provide an upward trend in $\delta M_r'$ until the end of March, the sustained negative δT_f (cf. Fig. 1) actually drives $\delta M_r'$ to lower values over this period. In April, the positive trend provided by δT_m finally reverses, while the cumulative effects of δT_f level off. (Superposed on these monthly trends, there are higher-frequency fluctuations in $\delta M_r'$ clearly related to δT_m that need not concern us here.) At the end of April, changes in $\delta M_r'$ due to δT_f are much larger than those due to δT_m, with $\delta M_r'$ and δT_f signals substantially above the residual level. Again, contributions from δT_g are negligible throughout the period. The picture emerging from Fig. 3a is, thus, one of dominant contributions by δT_f to the decline in M_r, which offset an opposite but weaker trend in δT_m, particularly until the end of March.

To examine regional contributions to the δT_f curve in Fig. 3a, time-integrated, zonally averaged τ_f anomalies were calculated over 46 equal-area latitudinal belts, as used in previous studies (Rosen 1993). A Hovmöller diagram of these anomalies in time and latitude is displayed in Fig. 3b for the period of interest. A strong negative anomaly in angular momentum transfer occurs over the northern subtropics, with maximum amplitudes centered at around 30°N. By the end of March, the cumulative effects of $\delta\tau_f$ near 30°N are more than twice as large as those at any other latitude. The northern subtropics are, thus, the region of most intense anomalous frictional transfers of AAM, leading to the decline of M_r to near-normal values by April 1983. Analysis of the longitudinal dependence of $\delta\tau_f$ (Fig. 4) indicates that most of these transfers are due to anomalous surface westerlies over the North Pacific, east of the date line.

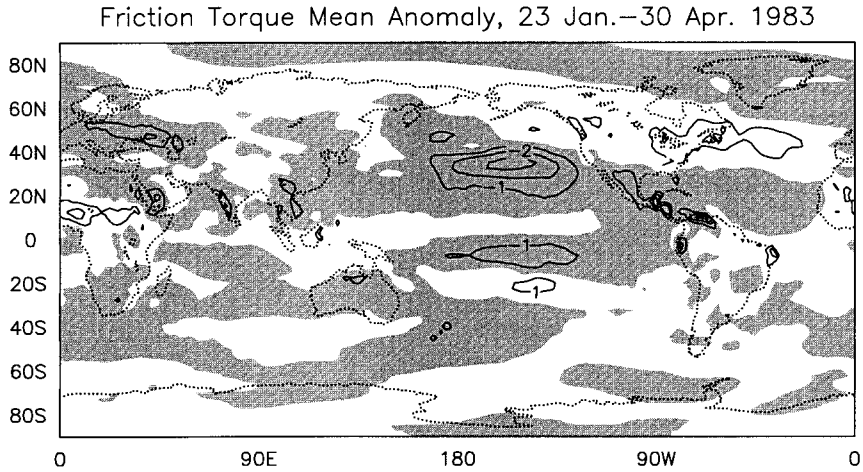

FIG. 4. Time-averaged anomalies in τ_f for the period 23 Jan–30 Apr 1983. Contour interval is 1×10^{16} kg m^2 s^{-2}; negative values are shaded.

4. Discussion and final remarks

Results in Figs. 2 and 3 point to the importance of northern latitude signals in the anomalous evolution of AAM during the 1982–83 El Niño. We begin the discussion with the January peak in AAM, corresponding to a strengthening of the tropical and subtropical westerlies in the Northern Hemisphere (Rosen et al. 1984) and mainly related to mountain torques on NA and EA orography. The importance of AAM exchanges over NA in our data agrees in general with the findings of Wolf and Smith (1987), who highlight the role of synoptic-scale systems in these exchanges. The development and tracks of these synoptic systems during January were related to the establishment of an unusually strong tropical–Northern Hemisphere (TNH) teleconnection pattern (Barnston and Livezey 1987), marked by negative height anomalies over the northeast Pacific and positive anomalies over subtropical North Pacific and mid-North America. Hoerling and Kumar (1997) succeed in reproducing much of this pattern's amplitude during northern winter 1982–83 with a general circulation model driven by realistic sea surface temperatures, thus suggesting that this manifestation of the TNH teleconnection pattern and the related synoptic activity involved in AAM exchanges over North America were intrinsic aspects of the 1982–83 El Niño.

The significant role we find for mountain torques on EA orography in also explaining the 23 January maximum in AAM is not mirrored, however, in the results of Wolf and Smith. Although NA torques are very important in both studies for the initial rise (~15–18 January), our Fig. 2 indicates a substantial contribution from EA torques starting around 18 January and lasting for several days. On the other hand, the mountain torques in Wolf and Smith over this period, with or without contributions from the Tibetan Plateau (see their Figs. 2 and 3), imply a (small) decrease in AAM, contrary to its observed behavior. Differences in methodology and datasets may account for this disagreement between the two studies, but our result is consistent with the movement, clearly visible on surface weather maps (not shown), of a synoptic-scale high pressure system to the east of the Tibetan Plateau over this period.

That the combined action of torques over separate mountain ranges is capable of producing rather large changes in AAM over short periods has been recently highlighted in another context (Iskenderian and Salstein 1998). During January 1983, the NA mountain torque is readily traced to the El Niño event, as discussed above, but the extent to which climate anomalies over Eurasia can also be linked to tropical sea surface temperatures has yet to be determined. Thus, Hoerling and Kumar (1997) are unable to reproduce important features observed over Eurasia in their simulation of the atmosphere's response to the 1982–83 El Niño. If, rather than also being driven by the El Niño, synoptic developments over Eurasia during January 1983 were merely fortuitously timed with respect to events occurring around North America, then this circumstance would help explain the difficulty in simulating the rapid AAM rise in the model experiments considered by Ponte et al. (1994). An alternate explanation may lie in their model's failure to capture the full intensity of the anomalies observed in the North American sector during January 1983 (Boer 1985).

Turning to the decrease of AAM to near-normal values depicted in Fig. 3, the anomalous frictional transfers of AAM over the subtropical Pacific are clearly related to the large-scale response of the atmosphere to El Niño conditions in the Tropics, that is, the TNH teleconnection pattern. In particular, large westerly anomalies throughout the troposphere in the subtropical northeast Pacific were associated with the near-record negative height and sea level pressure anomalies that formed over the Gulf of Alaska during 1982–83 northern winter (Quiroz 1983). These westerly anomalies remained

strong through March but decreased markedly in April 1983 (Chen 1983). The importance of frictional transfers over the ocean found here (cf. Fig. 4), together with the close relationship between AAM and length of day described by Rosen et al. (1984), brings into light anew the role of the ocean as a rapid conveyor of angular momentum between atmosphere and solid earth (Ponte 1990).

The relation of the friction torque anomalies in Figs. 3b and 4 with the large-scale subtropical westerly anomalies is clear, but we note that the synoptic-scale activity over the northeast Pacific during January 1983 continued with unusual intensity into February and March (Quiroz 1983; Chen 1983). These storms involved strong friction stress signals, which are clearly seen in Hovmöller diagrams of $\delta\tau_f$ (not shown). The signatures of these storms, involving negative (positive) $\delta\tau_f$ south (north) of $\sim$35°N, are superimposed on a background $\delta\tau_f$ signal determined by the large-scale flow. Whether these individual storm events provide a net frictional source or sink of AAM, besides any mountain torque anomalies that they may impart, remains an interesting question for future study.

Although anomalies in AAM during the 1982–83 El Niño have been linked primarily with jet stream signals at upper-tropospheric levels, these anomalies must be ultimately connected to the lower boundary where external torques act to remove or add AAM. So, for example, this and previous studies (e.g., Salstein and Rosen 1994) have established that the interaction of synoptic systems with large mountains can lead to regional torque signals that correlate well with global AAM tendencies, but details about the connection between the torque and AAM signals remain unclear (but see Czarnetzki 1997). In particular, the implicit angular momentum transports within the atmosphere have not been elucidated. Judging from the similar latitudes at which the torques and the main AAM changes seem to occur, local vertical transfers, through either eddy processes or enhanced mean meridional circulations, may be quite important. Regional angular momentum budgets seem in order to understand the dynamics supporting these vertical momentum transports.

In light of our results, the evolution of AAM during the 1982–83 El Niño involves a complex interplay of mountain and friction torques on various timescales and spatial scales. The relevance of this scenario to the description of AAM anomalous signals during other El Niño events remains to be seen. Of particular interest is the evolution of AAM during the recent, strong 1997–98 El Niño. Analyses of this event, currently being pursued by many researchers, will add to understanding of AAM behavior during extreme El Niño episodes.

Acknowledgments. We are grateful to K. Weickmann for providing the torque dataset and for useful clarifications on its contents. The invaluable assistance of P. Nelson in handling the data, performing all calculations, and drafting the figures for the paper is acknowledged. Support for this research has been provided by the Climate Dynamics Program of the U.S. National Science Foundation under Grant ATM-9632559 and the NASA Solid Earth and Natural Hazards Program under Contract NAS5-97269.

REFERENCES

Barnston, A., and R. E. Livezey, 1987: Classification, seasonality, and persistence of low-frequency circulation patterns. *Mon. Wea. Rev.,* **115,** 1083–1126.

Boer, G. J., 1985: Modeling the atmospheric response to the 1982/83 El Niño. *Coupled Ocean–Atmosphere Models,* J. C. J. Nihoul, Ed., Elsevier, 7–17.

——, 1990: The earth–atmosphere exchange of angular momentum simulated in a model and implications for the length of day. *J. Geophys. Res.*, **95,** 5511–5531.

Chen, W. Y., 1983: The climate of spring 1983—A season with persistent global anomalies associated with El Niño. *Mon. Wea. Rev.*, **111,** 2371–2384.

Czarnetzki, A. C., 1997: Regional mountain torque estimates over the Rocky Mountains in lee cyclones. *J. Atmos. Sci.*, **54,** 1986–1997.

Hoerling, M. P., and A. Kumar, 1997: Origins of extreme climate states during the 1982–83 ENSO winter. *J. Climate,* **10,** 2859–2870.

Huang, H.-P., P. D. Sardeshmukh, and K. M. Weickmann, 1999: The balance of global angular momentum in a long-term atmospheric data set. *J. Geophys. Res.*, **104,** 2031–2040.

Iskenderian, H., and D. A. Salstein, 1998: Regional sources of mountain torque variability and high-frequency fluctuations in atmospheric angular momentum. *Mon. Wea. Rev.,* **126,** 1681–1694.

Madden, R. A., and P. Speth, 1995: Estimates of atmospheric angular momentum, friction, and mountain torques during 1987–1988. *J. Atmos. Sci.*, **52,** 3681–3694.

Ponte, R. M., 1990: Barotropic motions and the exchange of angular momentum between the oceans and solid earth. *J. Geophys. Res.*, **95,** 11 369–11 374.

——, R. D. Rosen, and G. J. Boer, 1994: Angular momentum and torques in a simulation of the atmosphere's response to the 1982–83 El Niño. *J. Climate*, **7,** 538–550.

Quiroz, R. S., 1983: The climate of the ''El Niño'' winter of 1982–83—A season of extraordinary climatic anomalies. *Mon. Wea. Rev.*, **111,** 1685–1706.

Rosen, R. D., 1993: The axial momentum balance of earth and its fluid envelope. *Surv. Geophys.*, **14,** 1–29.

——, D. A. Salstein, T. M. Eubanks, J. O. Dickey, and J. A. Steppe, 1984: An El Niño signal in atmospheric angular momentum and Earth rotation. *Science*, **225,** 411–414.

Salstein, D. A., and R. D. Rosen, 1994: Topographic forcing of the atmosphere and a rapid change in the length of day. *Science*, **264,** 407–409.

——, and ——, 1997: Global momentum and energy signals from reanalysis systems. Preprints, *Seventh Conf. on Climate Variations*, Long Beach, CA, Amer. Meteor. Soc., 344–348.

Swinbank, R., 1985: The global atmospheric angular momentum balance inferred from analyses made during FGGE. *Quart. J. Roy. Meteor. Soc.*, **111,** 977–992.

Wolf, W. L., and R. B. Smith, 1987: Length-of-day changes and mountain torque during El Niño. *J. Atmos. Sci.*, **44,** 3656–3660.